Hindawi
Advances in Materials Science and Engineering
Volume 2018, Article ID 4081264, 8 pages
https://doi.org/10.1155/2018/4081264

Research Article

Simulation of Bending Fracture Process of Asphalt Mixture Semicircular Specimen with Extended Finite Element Method

Tian Xiaoge, Ren Zhang, Zhen Yang, Yantian Chu, Shaohua Zhen, and Yichao Xv

School of Traffic & Transportation Engineering, Changsha University of Science & Technology, 960 Wanjiali Road, Tianxin District, Changsha, Hunan 410114, China

Correspondence should be addressed to Tian Xiaoge; tianxiaoge@126.com

Received 2 May 2018; Accepted 23 September 2018; Published 17 October 2018

Academic Editor: Wei Zhou

In order to numerically simulate the whole fracture process including the initiation and propagation of crack in asphalt concrete semicircular specimens under external force, the extended finite element method (XFEM) was adopted considering the shortcomings of the conventional finite element method (FEM). The fracture processes of the semicircular specimens under 5 kinds of loading modes, M_e, were analyzed, and the simulation results were compared to the actual fracture paths in the actual specimens. The results indicated that the critical effective stress intensity factor will decrease first and then increase with the increase of M_e, and the XFEM simulation results are similar to that of the actual specimens in crack initiation angle and propagation path in the 5 different loading modes. It is proved that the XFEM is very effective in simulating the fracture process and has obvious advantages compared with the FEM. According to the stress state at the crack tip, the initiation angle and its propagation paths were analyzed, and it was pointed out that the increase of the shear stress component caused the crack initial angle to increase with the increase of M_e.

1. Introduction

Cracking is one of the most important and common forms of damage in asphalt pavement. It will not only destroy the integrity of the pavement structure, which will affect the pavement structural bearing capacity, but also it will reduce smoothness of the pavement surface, which will affect the driving quality and travelling comfort. Besides, rain and snow water will also penetrate into the inner of the pavement structure, which will induce water damage, so accelerate destruction of the pavement structure [1]. So, research in the crack initiation and propagation process until fracture completely of asphalt concrete under external action is of great significance, which will help to improve the crack resistance of asphalt concrete in the selection of raw materials, gradation optimization design, toughening, and crack resistant design. The expansion of cracks in three-dimensional structures along curved or tortuous paths is a thorny problem in structural numerical analysis. The assumption in traditional fracture mechanics that cracks are straight is no longer valid. Therefore, various analytical methods for crack in traditional fracture mechanics are helpless. The application of computational mechanics to simulate the random propagation of cracks in three-dimensional solid has become a hot topic in this field [2].

Owing to its great flexibility and applicability, the FEM has been widely used in numerical simulation of various fracture mechanics. However, it uses continuous function as the geometric interpolation function and stipulates that the material properties cannot mutate within the unit. So, the FEM is a suitable numerical method for continuum analysis, but there are some limitations in analyzing discontinuities such as cracks [2].

At present, the commonly used analysis methods of fracture mechanics are traditional FEM and adaptive grid [3], nodal force release method [4], cohesive force model [5], and embedded discontinuous model [6]. However, these methods have some limitations when dealing with complex shape cracks; for example, the crack propagation path must be given in advance and the crack can only extend along the cell boundary.

To overcome the shortcomings of the FEM, the XFEM was proposed by Belytschko and Black in 1999. The XFEM is based on the conventional FEM and fracture mechanical theory. It is a new method to analyze complex fracture problem. Jump function and gradual displacement shape function at the crack tip were introduced to characterize the discontinuity between two surfaces of the crack. So, the inconvenience caused by remeshing the crack tip was avoided when the fracture problem is calculated using the conventional FEM. So, the XFEM has significant advantages in solving the effect of crack initiation and its propagation. So, it becomes a hot topic in mechanical research at home and abroad [2].

Pu and Manhan analyzed the extension of cracking in asphalt concrete overlay on cement concrete pavement using the XFEM [7]. Wang et al. analyzed crack propagation characteristics of asphalt mixture with the basalt fiber utilizing the XFEM [8]. Zhang et al. analyzed the two-dimensional expansion of surface cracks in asphalt pavement using the XFEM [9]. Xigang analyzed temperature cracks in asphalt pavement using the XFEM [10], and Pirmohammad and Ayatollahi analyzed the fracture toughness of asphalt concrete in different loading modes [11]. Zhang et al. simulated the propagation process of cracking in the cement concrete specimen with the XFEM [12]. Aliha et al. investigated the mixed mode I/II crack growth behavior of a sedimentary soft rock (Guiting limestone) experimentally and theoretically using both the centre cracked circular disc (CCCD) and the edge cracked semicircular bend (SCB) specimens [13]. Pook studied a collection of case on fatigue crack paths observed in metallic materials [14]. Shahani and Tabatabaei assessed the effect of specimen geometry on the T-stress value and effect of T-stress on different fracture criteria [15]. Sajjadi et al. proposed a novel mixed mode brittle fracture criterion for crack growth path prediction under static and fatigue loading [16]. Berto and Gomez investigated the possibility to use two fracture criteria in mixed mode fracture of notched components [17]. Matvienko and Morozov predicted the angle of surface crack growth under conditions of rolling-sliding using incremental method and integral (global) method [18]. Matvienko proposed the maximum average tangential stress (MATS) criterion for predicting the direction of fracture angle [19]. In this paper, the XFEM was utilized to analyze the fracture process and its path in asphalt concrete semicircular specimens under different loading modes.

2. Basic Principles of the XFEM

The analysis domain as shown in Figure 1 can be divided into three different regions: the continuous region, crack tip region, and crack fully penetrated region.

For the continuous region, the same method used in the ordinary FEM is used in the XFEM. For the crack and adjacent regions, due to the existence of discontinuity in displacement, stress and strain in the element, and stress concentration at the crack tip, an extended shape function should be introduced to deal with them.

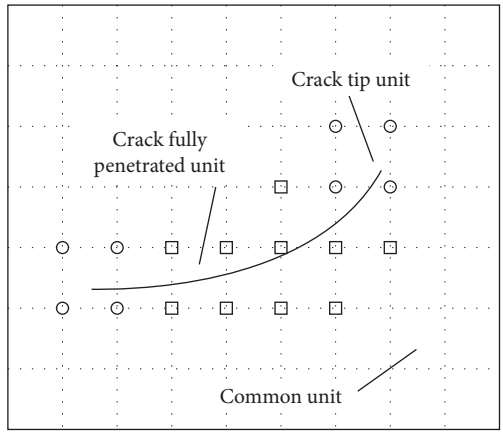

Figure 1: Analysis domain including a crack.

In the conventional FEM, the shape function is shown as follows:

$$u = \sum_I N_I(x) u_I, \tag{1}$$

where N_I is the interpolation shape function of the node I and u_I is the displacement vector of the node I.

This kind of displacement mode is only applicable to units in the continuous region, but it is no longer suitable when the unit is discontinuous, such as unit containing cracks and/or holes.

Based on the conventional finite element method, an extended and discontinuous shape function was introduced in the XFEM to more accurately describe the discontinuities in the computational domain. In the XFEM, the unknown field u^h is composed of two parts:

$$u^h = \sum_I N_I(x) u_I + \psi(x), \tag{2}$$

where $N_I(x)$ is the shape function of the node I in the conventional FEM and u_I is the degree of freedom at the node I. Both $N_I(x)$ and u_I are the same as in the FEM.

The expansion term $\psi(x)$ is used to improve the quality of characterizing of the unknown field. In the construction of the function $\psi(x)$, certain characteristics of the true solution of the unknown field, u^h, should be introduced to increase the convergence speed. In fact, it is often constructed based on the solution space of the real solution.

According to the properties of partition of unity, formula (2) can be further expressed as

$$u^h = \sum_I N_I(x) u_I + \sum_J N_J(x) \Phi(x) q_J. \tag{3}$$

Let $\psi_J(x) = N_J(x)\Phi(x)$, so

$$u^h = \sum_I N_I(x) u_I + \sum_J \psi_J(x) q_J. \tag{4}$$

Equation (3) or (4) is the approximate scheme of the shape function used in the XFEM. Compared with the conventional FEM, the biggest difference is the introduction of redundant degree of freedom at element nodes.

(1) For the fully penetrated crack unit, there is an abrupt change in the displacements on both sides of the crack, and the extended shape function $\psi_J(x)$ can be composed as

$$\psi_J(x) = N_J(x) \times H(f(x)), \tag{5}$$

where $H(x)$ is the step function and $f(x)$ is the level set function. They are expressed as Equations (6) and (7), respectively:

$$H(x) = \begin{cases} 1, & x \geq 0, \\ -1, & x < 0, \end{cases} \tag{6}$$

$$f(x) = \min\|x - \overline{x}\| \times \operatorname{sign}\left(n^+ \cdot (x - \overline{x})\right), \tag{7}$$

where n^+ is the unit normal vector on a broken line, such as crack. For any node that is not on the broken line, $f(x)$ is the shortest distance from the node x to the broken line. And, if the location of a node x is coinciding with the direction of n^+, $f(x)$ takes a positive value. Or else, then $f(x)$ takes a negative value.

(2) The extended shape function $\psi_J(x)$ for nodes around the crack tip can be composed as follows:

$$\psi_J(x) = N_J(x) \times \Phi(x), \tag{8}$$

where $\Phi(x)$ can be a linear combination of the following function basis:

$$\Phi(x) = \left[\sqrt{r}\,\sin\frac{\theta}{2},\ \sqrt{r}\,\sin\frac{\theta}{2}\sin\theta,\ \sqrt{r}\,\cos\frac{\theta}{2},\ \sqrt{r}\,\cos\frac{\theta}{2}\sin\theta \right]. \tag{9}$$

In fact, the expansion function basis of $\Phi(x)$ is exactly the analytical displacement solution at the crack tip of the plane composite crack in linear elastic fracture mechanics [20]. The shape function of the crack tip composed with them can not only express the discontinuous property of the displacement at the crack but also accurately capture the displacement field at the crack tip. Actually, it is the reason that some information of the known solutions (such as physical properties of the obtained solution or partial analytical solution) were composed into the extended shape function. The XFEM can not only improve calculation accuracy but also significantly reduce the computation time.

So, the extended displacement mode, Equation (10), was introduced in the XFEM to describe the approximate displacement interpolation function for elements in the crack regions:

$$u = \sum_{i=1}^{N} N_I(x)\left[u_I + H(x)a_I + \sum_{\alpha=1}^{4} F_\alpha(x) b_I^\alpha\right]. \tag{10}$$

Based on the conventional FEM, the process on crack analysis in the XFEM was divided into two parts:

(1) Meshing the whole domain while ignoring the inner boundary: cracks can pass across the unit, regardless of the boundary constraints of the unit.

(2) Extended shape function, formula (10), was used to improve the approximation space of the finite element. The other analytical processes are the same of the conventional FEM.

3. Bending Fracture Tests of Asphalt Mixture Semicircular Specimens

Semicircular specimens with prefabricated cracks were selected to conduct bending fracture tests at −15°C to study the fracture resistance of asphalt concrete AC-13 under five different loading modes.

The gradation of asphalt mixture AC-13 is shown in Table 1. The materials used were basalt aggregates, limestone powder, and AH70 asphalt. The optimal asphalt-aggregate ratio of 5.3% was determined through Marshall tests [21].

The radius, R, of the specimens is 150 mm and their thickness, t, is 32 mm and the length of prefabricated crack, a, is 20 mm and its width, b, is 1.5 mm.

The different fracture loading modes at the tip of prefabricated crack are achieved through adjusting the locations (S_1 and S_2) of 2 bearings and the location of prefabricated crack (L), which are shown in Figure 2 and Table 2 [22]. The loading rate was controlled at 3 mm/min with MTS810.

The parameter, M_e, is the fracture loading mode with different positions of bearings, S_1 and S_2, and prefabricated crack L.

The bending fracture tests of semicircular specimens were conducted with a servohydraulic test machine, MTS at the temperature of −15°C. Before the test, specimens were kept at −15°C for 4 hours in the environmental chamber to ensure that both the inside and outside of the specimen achieved the setting test temperature, −15°C. Then, the specimen was installed according to the locations of the bearing points in Table 2, and three point bending fracture tests were carried out. The loading rate was controlled with displacement increment at 3 mm/min. The data acquisition system collects force and displacement with time during the loading process, and the time interval of data acquisition is 0.01 s. After the test, the critical effective stress intensity factors (K_{eff}) are calculated using Equation (11) according to the maximum load P_{cr}, obtained from the tests:

$$\begin{aligned} K_{\text{I}f} &= Y_{\text{I}} \frac{P_{\text{cr}}}{2Rt}\sqrt{\pi a}, \\ K_{\text{II}f} &= Y_{\text{II}} \frac{P_{\text{cr}}}{2Rt}\sqrt{\pi a}, \\ K_{\text{eff}} &= \sqrt{K_{\text{I}f}^2 + K_{\text{II}f}^2}, \end{aligned} \tag{11}$$

where $K_{\text{I}f}$, $K_{\text{II}f}$, and K_{eff} are the critical effective stress intensity factors under the pure bending fracture mode, mode I, pure shear fracture mode, mode II, and mixed fracture mode, mixed mode I/II, respectively.

Table 1: Gradation of AC-13.

Sieve size (mm)	31.5	26.5	19	16	13.2	9.5	4.75	2.36	1.18	0.6	0.3	0.15	0.075
Passing rate (%)	100	100	100	100	95.2	71.8	51.6	32.9	23.6	18.3	12.1	9.3	5.8

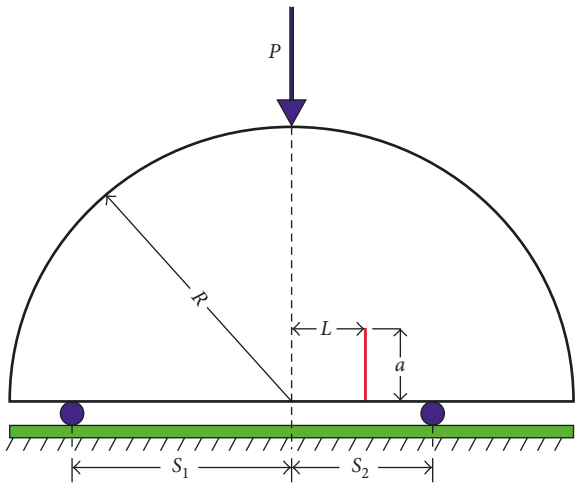

Figure 2: Positions of bearings and prefabricated crack in specimen.

Table 2: Positions of bearings and prefabricated crack at different loading modes.

Loading mode	S_1 (mm)	S_2 (mm)	L (mm)	M_e
Pure bending mode, I	50	50	0	1.0
	50	20	−2	0.8
Mixed loading mode, I/II	50	20	5	0.5
	50	20	11	0.2
Pure shear mode, II	50	20	16	0

Y_I and Y_{II} are geometric parameters reflecting the influence of the size and shape of the specimen, the position, length, and width of the prefabricated crack to the stress intensity factor. The values of Y_I and Y_{II} for different specimens and different fracture modes are listed in Table 3.

According to the above test plan, the critical effective stress intensity factor, K_{eff}, of asphalt concrete AC-13 at −15°C under different loading modes were obtained.

3.1. The Effect of Loading Mode on the Initial Angle and Propagation Path of the Crack. The fracture propagation paths at the surface of the specimens under different loading modes are shown in Figure 3.

It can be seen from Figure 3 that the crack is initiating and propagating upward basically along the direction of the prefabricated crack in a straight line under the pure bending fracture mode, mode I (Figure 3(a)). But under other loading modes, pure shear mode, mode II, and 3 mixed modes I/II, the cracks initiate at a certain angle (which was named initiation angle) to the direction of the prefabricated crack, and then, they are propagating upward in a form of curves, finally arrived at the loading position (Figures 3(b)–3(e)).

With the decrease of the load mode parameter M_e, the values of initiation angle increases. The reason is that the horizontal tensile stress is the only action at the crack tip under the fracture mode I, the direction of the principal stress is the direction of horizontal tensile stress, so, the crack will initiate and propagate along the direction of the crack. But in the other modes (mode II or mixed mode I/II), there is the action of shear stress besides of horizontal tensile stress, so, the direction of principal stress is no longer perpendicular to the prefabricated crack surface. So, the crack will initiate at an angle to the prefabricated crack surface. The angle is named initiation angle. The value of the initiation angle is related to the relative value of the horizontal tensile stress and shear stress. The shear stress component increases with the decrease of the loading mode, M_e. And the relative values of shear stress to the horizontal tensile stress increase. So, the crack initial angle increases with the decrease of the loading mode, M_e.

3.2. Variation of Critical Stress Intensity Factor with the Fracture Mode. The fracture load, P_{cr}, at different loading modes, M_e, is shown in Table 4, and the values of critical effective stress intensity factor (SIF) K_{eff} at different loading mode M_e were calculated and are shown in Table 4 and Figure 4.

It can be seen visually from Figure 4 that the critical effective stress intensity factor, K_{eff}, will decrease firstly and then increase with the increase of the load model parameter, M_e.

The critical effective stress intensity factor, K_{eff}, under mode I and mode II, is greater than the value of K_{eff} under all mixed loading modes. The minimum value of K_{eff} is obtained when the loading mode parameter M_e is 0.8.

4. Simulation of Bending Fracture Process in the Specimens under Different Loading Modes

The XFEM was used to analyze the initialization and propagation process of the crack in AC-13 specimens under different loading modes.

At the temperature −15°C of the bending fracture test conducted, asphalt mixture, AC-13, can be seen as an elastic material. Its elastic modulus E is 10400 MPa and Poisson's ratio is 0.25, measured via compressing modulus test at −15°C. The parameters used in the XFEM program are shown in Table 5.

The maximum displacement is the displacement when the specimen is fractured completely.

In the XFEM program, the maximum principal stress criterion was selected for fracture criterion, and the

Table 3: The values of Y_I and Y_{II} for different specimens.

Loading mode	S_1 (mm)	S_2 (mm)	L (mm)	M_e	Y_I (MPa·m$^{1/2}$)	Y_{II} (MPa·m$^{1/2}$)
I	50	50	0	1.0	3.734	0
I/II	50	20	−2	0.8	1.655	0.546
I/II	50	20	5	0.5	1.171	1.131
I/II	50	20	11	0.2	0.599	1.792
II	50	20	16	0	0	2.298

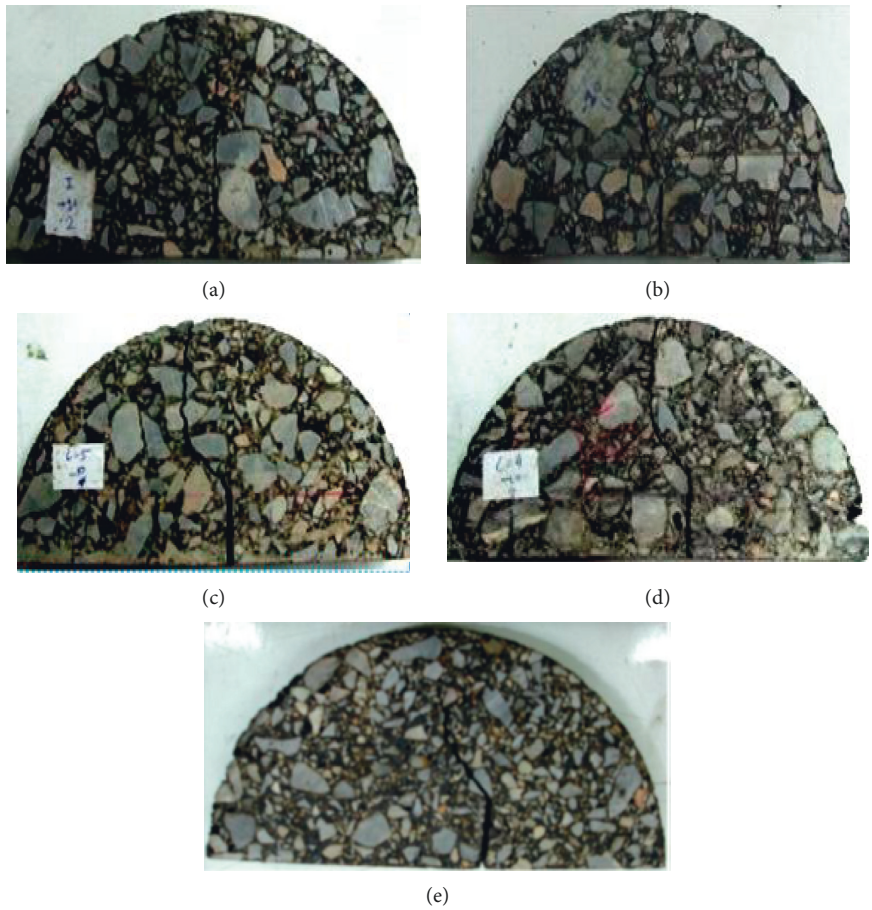

Figure 3: Crack routes at different loading modes. (a) M_e = 1.0. (b) M_e = 0.8. (c) M_e = 0.5. (d) M_e = 0.2. (e) M_e = 0.

displacement criterion was selected for damage evolution criterion.

4.1. Simulation of Fracture Process at Different Loading Modes

4.1.1. M_e = 1.0. The established plane strain model and its boundary conditions are shown in Figure 5. Its XFEM mesh is shown in Figure 6.

The simulation results of cracking in the XFEM are shown in Figure 7.

It can be seen from Figure 6 that the stress fields calculated with the XFEM are symmetrically distributed at the pure tension loading mode, Type I. During the crack growth, stress concentration occurs at the crack tip. It is not necessary to arrange a dense mesh at the crack tip or to continuously redraw the mesh to satisfy the crack propagation during the analysis.

Comparing Figures 7 and 3(a), it can be found that the fracture propagation path simulated through the XFEM is basically the same as that of the actual specimen.

4.1.2. M_e = 0.8. The calculation results are shown in Figure 8.

Comparing Figures 8 and 3(b), it can be seen that in the mixed loading mode (M_e = 0.8), the initiation of the crack is no longer along with the prefabricated crack. There is a certain angle to the direction of the prefabricated crack. And then propagate upward in a curved form. It can also be seen from Figure 8 that the distributions of horizontal tensile stress and shear stress are asymmetrical.

Table 4: Fracture loads and critical effective SIFs at different loading modes.

Loading mode	Maximum displacement (mm)	Fracture load, P_{cr} (kN)	Effective SIF, K_{eff} (MPa·m$^{0.5}$)
M_e = 1	0.286	7.51	1.46
M_e = 0.8	0.585	10.59	0.96
M_e = 0.5	0.497	13.57	1.15
M_e = 0.2	0.801	14.40	1.42
M_e = 0	1.025	15.55	1.87

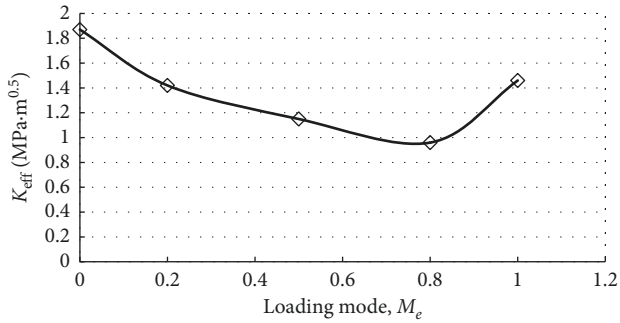

Figure 4: Variation of K_{eff} with loading mode M_e.

Table 5: Calculation parameters under different loading modes.

Loading mode, M_e	Maximum displacement (mm)	Loading speed	Elastic modulus, E (MPa)	Poisson's ratio
1	0.286			
0.8	0.585			
0.5	0.497	3 mm/min	10400	0.25
0.2	0.801			
0	1.025			

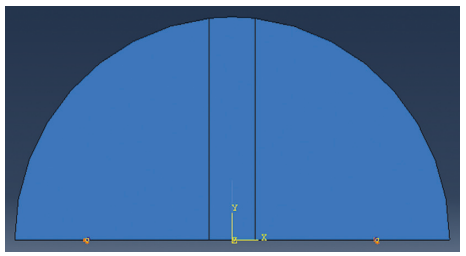

Figure 5: Geometric model and boundary conditions.

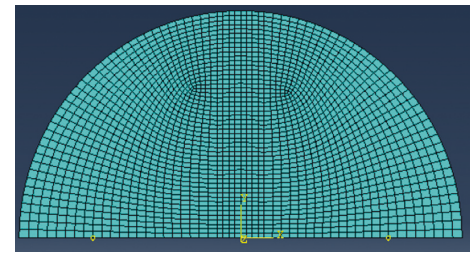

Figure 6: Mesh of XFEM.

Comparing Figures 8 and 3(b), the propagation paths of the crack are basically the same. The crack initiation angle (CIA) calculated with the XFEM is 29° and 30° in the actual specimen, which shows a good agreement.

4.1.3. M_e = 0.5. The calculation results are shown in Figure 9:

Comparing Figures 9 and 3(c), the expansion paths of the two are basically the same.

The CIA calculated with the XFEM is 33° and 32° in the actual fracture test, which shows a good agreement.

4.1.4. M_e = 0.2. The calculation results are shown in Figure 10:

Comparing Figures 10 and 3(d), the expansion paths of the two diagrams are basically the same.

The CIA calculated with the XFEM is 38° and 36° in the fracture test, which shows a good agreement.

4.1.5. M_e = 0. The calculation results are shown in Figure 11:

Comparing Figures 11 and 3(e), the crack expansion paths of the two diagrams are basically the same. The CIA calculated by the XFEM is 50° and 51° in the fracture test, which shows a good agreement.

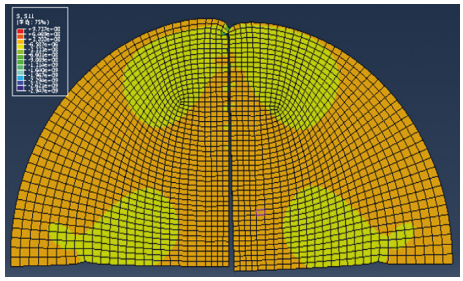

Figure 7: Crack propagation from XFEM.

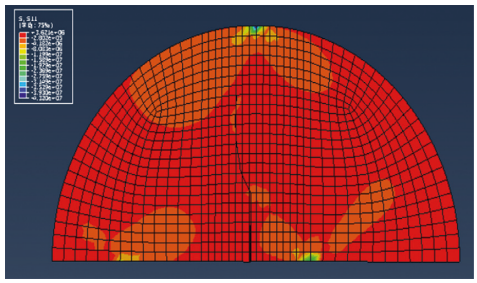

(a)

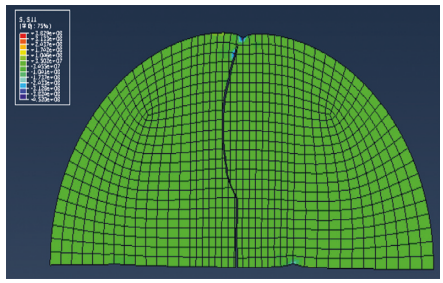

(b)

Figure 8: Distribution of stress and crack propagation process. (a) Horizontal tensile stress. (b) Shear stress.

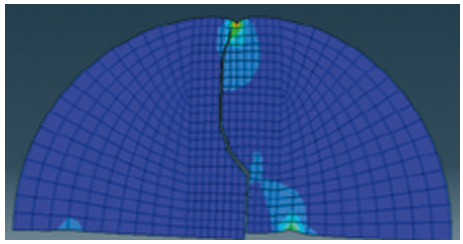

Figure 9: Distribution of stress and crack propagation path from XFEM.

4.2. The Variation of CIA to M_e. The calculated and measured crack initial angle (CIA) at crack tip under different loading modes are summarized in Table 6.

It can be seen from Table 6 that the calculated CIAs with the XFEM agree with the measured CIAs from the test. And the values of the CIA are increasing with the decrease of the loading mode. The reason is that the action of shear stress is stronger with the decrease of the loading mode, M_e.

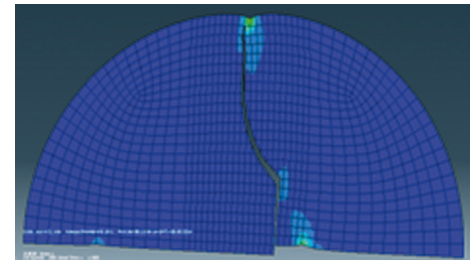

Figure 10: Distribution of stress and crack propagation path from XFEM.

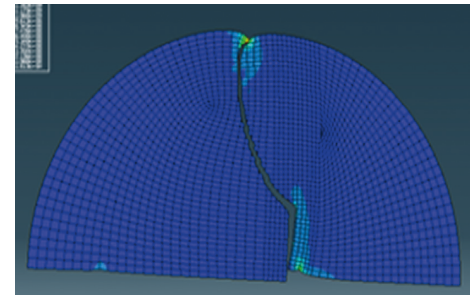

Figure 11: Distribution of stress and crack propagation path from XFEM.

Table 6: The CIA at different loading modes.

Loading mode, M_e	CIA (°)	
	Measured	Calculated with XFEM
1.0	0	0
0.8	30	29
0.5	32	33
0.2	36	38
0	51	50

5. Conclusion

In this paper, the XFEM was used to simulate the fracture process in asphalt concrete AC-13 semicircular specimen under −15°C with different loading modes. The following results were obtained:

(1) The critical effective stress intensity factor, K_{eff}, is decreasing firstly and then increasing with the decrease of the loading mode, M_e. And the minimum K_{eff} is achieved when the $M_e = 0.8$.

(2) The crack initiation angle (CIA) and propagation path varied with the loading mode. At the pure bending mode, the value of the CIA is 0° and it will propagate upward in a linear path, whereas under other loading modes, there is a certain angle between the cracking direction and the direction of the prefabricated crack. And then the crack propagates upward in a curved path because of the effect of shear stress at the crack tip.

(3) Under different loading modes, the crack shape, cracking propagation angle (CPA), crack propagation shape, and crack path curve of the XFEM simulation are in good agreement with those in the actual specimens, which indicated that the XFEM can be used well to calculate the crack effect and its propagation in the asphalt mixture specimen.

(4) The crack initiation angle is increased with the decrease of the value of the loading mode, M_e. This is due to the increasing effect of shear stress in the load.

Data Availability

The data used to support the findings of this study are available from the corresponding author upon request.

Conflicts of Interest

The authors declare that there are no conflicts of interest regarding the publication of this paper.

Acknowledgments

The authors appreciate the support of the National Natural Science Foundation of China (50878032).

References

[1] K. Majidzadeh, E. M. Kauffmann, and D. V. Ramsamooj, "Application of fracture mechanics in the analysis of pavement fatigue," *Journal of Asphalt Pavement Technology*, vol. 40, pp. 227–246, 1971.

[2] Z. Zuo, Z. Liu, B. Cheng et al., *Extended Finite Element Method*, Tsinghua University Press, Beijing, China, 2012.

[3] C. Miehe and E. Gurses, "A robust algorithm for configurational force driven brittle crack propagation with R adaptive mesh alignment," *International Journal for Numerical Methods in Engineering*, vol. 72, no. 2, pp. 127–155, 2007.

[4] Z. Zhuang and P. E. O'Donoghue, "The recent development of analytical methodology for crack propagation and arrest in the gas pipelines," *International Journal of Fracture*, vol. 101, no. 3, pp. 269–290, 2000.

[5] X. P. Xu and A. Needleman, "Numerical simulations of fast crack growth in brittle solids," *Journal of the Mechanics and Physics of Solids*, vol. 42, no. 9, pp. 1397–1434, 1994.

[6] T. Belytschko, J. Fish, and B. E. Engelmann, "A finite element with embedded localization zones," *Computer Methods in Applied Mechanics and Engineering*, vol. 70, no. 1, pp. 59–89, 1988.

[7] P. Pu and S. Manhan, "Fracture propagation in asphalt overlay based on XFEM," *Highway Engineering*, vol. 37, no. 4, 2012.

[8] S. Wang, Y. Zhao, and L. Zhao, "Analysis of crack propagation characteristics of basalt mineral fiber asphalt mixture by using the extended finite element method (XFEM)," *China Science and Technology Information*, vol. 08, 2013.

[9] Z. Zhang, F. Li, Q. Yang et al., "Two-dimensional surface crack propagation in asphalt pavement using XFEM," *Chinese Journal of Civil Engineering and Management*, vol. 28, no. 2, 2011.

[10] Z. Xigang, *Finite Element Analysis of Temperature Crack in Asphalt Surface*, Zhengzhou University, Zhengzhou, China, 2012.

[11] S. Pirmohammad and M. R. Ayatollahi, "Fracture resistance of asphalt concrete under different loading modes," *Construction and Building Materials*, vol. 53, pp. 235–242, 2014.

[12] X. Zhang, Y. Ding, and X. Ren, "Extension finite element method simulation of crack propagation process in concrete," *Journal of Engineering Mechanics*, vol. 30, no. 7, 2013.

[13] M. R. M. Aliha, M. R. Ayatollahi, D. J. Smith, and M. J. Pavier, "Geometry and size effects on fracture trajectory in a limestone rock under mixed mode loading," *Engineering Fracture Mechanics*, vol. 77, no. 11, pp. 2200–2212, 2010.

[14] L. P. Pook, "The linear elastic analysis of cracked bodies, crack paths and some practical crack path examples," *Engineering Fracture Mechanics*, vol. 167, pp. 2–19, 2016.

[15] A. R. Shahani and S. A. Tabatabaei, "Effect of T-stress on the fracture of a four point bend specimen," *Materials & Design*, vol. 30, no. 7, pp. 2630–2635, 2008.

[16] S. H. Sajjadi, M. J. Ostad Ahmad Ghorabi, and D. Salimi-Majd, "A novel mixed-mode brittle fracture criterion for crack growth path prediction under static and fatigue loading," *Fatigue & Fracture of Engineering Materials & Structures*, vol. 38, no. 11, pp. 1372–1382, 2015.

[17] F. Berto and J. Gomez, "Notched plates in mixed mode loading (I + II): a review based on the local strain energy density and the cohesive zone model," *Engineering Solid Mechanics*, vol. 2017, pp. 1–8, 2017.

[18] Y. G. Matvienko and E. M. Morozov, "Two basic approaches in a search of the crack propagation angle," *Fatigue & Fracture of Engineering Materials & Structures*, vol. 40, no. 8, pp. 1191–1200, 2017.

[19] Y. G. Matvienko, "Maximum average tangential stress criterion for prediction of the crack path," *International Journal of Fracture*, vol. 176, no. 1, pp. 113–118, 2012.

[20] Z. Wang and S. Chen, *Advanced Fracture Mechanics*, Science Press, Beijing, China, 2009.

[21] JTGD50-2006, *Chinese Design Specifications of Highway Asphalt Pavement*, China Communications Press, Beijing, China, 2006.

[22] X. Tian, H. Han, X. Li et al., "Study on fracture characteristics of asphalt concrete under different loading modes," *Journal of Building Materials*, vol. 98, no. 4, pp. 150–153, 2016.